

Reentrant transition and spin-glass state in $\text{CdCr}_{2x}\text{In}_{2-2x}\text{Se}_4$ thin films

M. Lubecka and L. J. Maksymowicz

Institute of Electronics, Academy of Mining and Metallurgy, al. Mickiewicza 30, Krakow, Poland

(Received 21 February 1991)

Magnetic properties of polycrystalline thin films of chromium chalcogenide spinels, i.e., CdCr_2Se_4 lightly doped with indium and $\text{CdCr}_{2x}\text{In}_{2-2x}\text{Se}_4$, are studied. The ferromagnetic- and spin-wave-resonance techniques have been used to investigate the temperature dependences of the spin-wave stiffness constant D , the saturation magnetization M_s , and the resonance linewidth Γ . The resonance spectra have been recorded in the temperature range extending from 4.2 to 300 K. The influence of indium concentration on $M_s(T)$, $D(T)$, and $\Gamma(T)$ is studied. It is shown that lightly doped samples ($[\text{In}]/[\text{Cd}] < 1\%$) exhibit ferromagnetic ordering, with $M_s(T)$ and $D(T)$ being linear functions of $T^{3/2}$ and $T^{5/2}$, respectively. A higher concentration of indium produces the reentrant transition and spin-glass state of magnetic ordering in $\text{CdCr}_{2x}\text{In}_{2-2x}\text{Se}_4$. A numerical analysis of the saturation magnetization and linewidth temperature dependence has been performed in order to determine the type of magnetic ordering.

I. INTRODUCTION

The magnetic properties of CdCr_2Se_4 chalcogenide spinels are very sensitive to In doping.^{1,2} Our previous results,^{3,4} show that the magnetic properties of Cd-Cr-In-Se thin films strongly depend on indium concentration. Chromium spinels of $\text{CdCr}_2\text{Se}_4\text{:In}$ are classified as magnetic semiconductors. The magnetic properties of these samples indicate the ferromagnetic ordering below the Curie temperature T_C . Therefore, the temperature dependences of both the saturation magnetization M_s and the stiffness constant D can be described by the spin-wave theory.

The reentrant transition is obtained in $\text{CdCr}_{2x}\text{In}_{2-2x}\text{Se}_4$ at high concentration of indium ($0.85 \leq x < 1$).^{5,6} Further increase in In content ($x < 0.85$) results in the spin-glass behavior.

The experimental techniques involved in the measurements of the magnetic properties of thin films require higher sensitivities than standard methods applied in the studies of bulk ferromagnetism. The ferromagnetic resonance (FMR) and spin-wave resonance (SWR) techniques are of particular importance in the studies of the temperature dependences of magnetic parameters.

The SWR spectra with well-resolved volume modes can be obtained by low-energy excitations at the microwave frequency (the microwave spectrometer) for appropriate boundary conditions of surface spins. Then, a dispersion relation for volume modes may be used to calculate the exchange constant A .³ The saturation magnetization M_s and the stiffness constant D can be derived from the ferromagnetic resonance spectra in the perpendicular and parallel geometries.

II. EXPERIMENT

Thin CdCr_2Se_4 films lightly doped with In ($[\text{In}]/[\text{Cd}] < 1\%$) and $\text{CdCr}_{2x}\text{In}_{2-2x}\text{Se}_4$ with $0.7 < x < 1$

were deposited in a high vacuum system. Four independent sources of Cd, Cr, Se, and In were used during the evaporation process.⁷ Deposition rate was a known function of temperature of the sources. The three-layer structure was prepared as follows. A thin layer of Cr ($\approx 50\text{\AA}$) was deposited onto a Corning glass substrate preheated to about 420 K in order to improve the film adhesion. The Cd-Cr-Se-In film was evaporated at the substrate temperature of about 350 K onto the Cr layer. A thin layer of Cr was then deposited at 350 K in order to inhibit diffusion of Cd and Se during the subsequent annealing process. As-deposited samples were in the amorphous state. The film thickness was measured after deposition by means of Talysurf 4 profilometer. Thickness of the samples was also controlled during deposition process by the measurement of sample resistivity. The process of crystallization was studied in a Kristalloflex 4H x-ray-diffraction apparatus at different temperatures and for different annealing time intervals. The x-ray-diffraction patterns were recorded *in situ* after each stage of heat treatment had been completed. It was found that the samples reached the polycrystalline state after being annealed at 790 K for 1 h. The composition of samples was analyzed by means of an x-ray microprobe (ARL SEMQ microanalyzer) and Auger spectroscopy (Riber LAS-620).

The magnetic parameters of the samples such as the saturation magnetization M_s , g factor, both Curie and Curie-Weiss temperatures, the exchange interaction constant A , and the spin-wave stiffness constant D were found from the ferromagnetic resonance and spin-wave resonance. The microwave spectrometer at the X band was used for FMR and SWR experiments. The spectra were recorded in the temperature range 4.2–300 K. The external magnetic field was applied in the direction perpendicular to the film plane (perpendicular geometry) and in the direction parallel to the film plane (parallel geometry).

III. RESULTS AND DISCUSSION

The composition of the samples, i.e., the In doping level was intentionally varied in order to study (i) the ferromagnetic state (FM), (ii) the reentrant transition (REE), and (iii) the spin-glass state (SG).

(i) Ferromagnetic state. From the microscopic point of view, the FM state is expected at a very high spin concentration which produces the long-range spin correlation. The correlated spins form a so-called infinite ferromagnetic network (IFN).

The SWR was detected in thin films of CdCr_2Se_4 doped with In ($\text{Cd}_{0.99}\text{In}_{0.01}\text{Cr}_2\text{Se}_4$) in the temperature range from 30 to 110 K. It is well known that the SWR is observed when the surface spins satisfy the appropriate boundary conditions. The semiclassical approach, based on the Rado-Weertman model,⁸ yields $k = n\pi/L$ for a limiting case of completely pinned surface spins. Here, k is a wave vector of a microwave component of the magnetization, n is an odd integer, and L stands for a film thickness.

The dispersion relation for low-energy excited volume modes in a microwave spectrometry experiment, for the perpendicular geometry, can be expressed as^{3,4}

$$(\omega/\gamma)_\perp = H_n - 4\pi M_s + (2A/M_s)(n\pi/L)^2, \quad (1)$$

where $\omega = 2\pi\nu$, ν is the microwave frequency, and γ is the gyromagnetic factor.

For the uniform mode ($k = 0$)

$$(\omega/\gamma)_\perp = H_\perp - 4\pi M_s. \quad (2)$$

In the case of parallel geometry, we have

$$(\omega/\gamma)_\parallel^2 = [H_n + (2A/M_s)(n\pi/L)^2] \times [H_n + 4\pi M_s + (2A/M_s)(n\pi/L)^2]. \quad (3)$$

For the uniform mode, Eq. (3) reduces to

$$(\omega/\gamma)_\parallel^2 = H_\parallel(H_\parallel + 4\pi M_s). \quad (4)$$

The SWR experiment was performed for the perpendicular geometry. The exchange constant A was found from the best fit of the predicted quadratic dependence of H_n versus mode number n (see Fig. 1) to the experimental data. In the real case this dependence ($H_n \sim n^2$) cannot be used for lower-order modes because of the microscopic fluctuations of the magnetic parameters.

Figure 1 shows H_n as a function of n^2 for different temperatures. For higher-order modes, the linear relationship between H_n and n^2 is seen, thus allowing one to establish the value of $(2A/M_s)(\pi/L)^2$ from the slope of the line. The temperature dependences of the resonance field H_r of the uniform mode in the perpendicular and parallel geometries are presented in Fig. 2. Ferromagnetic-paramagnetic transition temperature, i.e., the temperature at which $H_\parallel = H_\perp$ can be derived easily from these data. From Eqs. (2) and (4), assuming that $(\omega/\gamma)_\perp = (\omega/\gamma)_\parallel$, one gets

$$4\pi M_s = H_\perp + 0.5H_\parallel - [H_\parallel(H_\perp + 1.25H_\parallel)]^{1/2}. \quad (5)$$

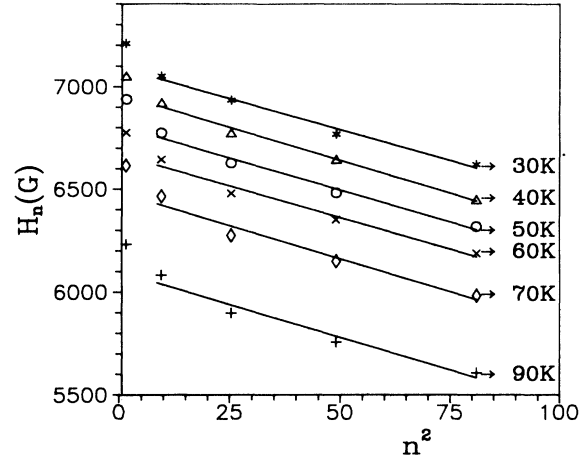


FIG. 1. The dependence of the resonance-field position H_n on the square of the mode number n^2 for a 5000-Å-thick $\text{CdCr}_2\text{Se}_4:\text{In}$ sample. Solid lines represent the linear best fit to the experimental data ($n=1$ was excluded from the fitting procedure). $A = (2.3 \pm 0.2) \times 10^{-12}$ J/m for $T=40$ K, $A = (2.4 \pm 2) \times 10^{-12}$ J/m for $T=50$ K.

The temperature dependence of M_s is obtained from the experimental data [Fig. 2 and Eq. (5)] presented above. Figure 3 shows M_s vs $T^{3/2}$ for a CdCr_2Se_4 thin film lightly doped with In. It is seen that Bloch's law holds. From the spin-wave theory,⁹ one expects

$$M_s(T) = M(0)(1 - BT^{3/2} - \dots). \quad (6)$$

The spin-wave stiffness constant D is related to B :

$$B = \xi(\frac{3}{2})[g\mu_B/M(0)](k_B/4\pi D)^{3/2}, \quad (7)$$

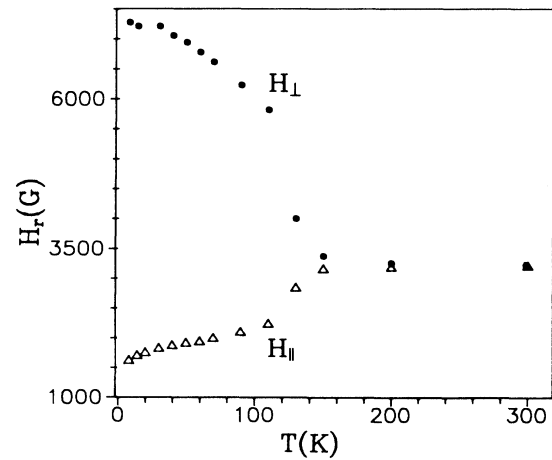


FIG. 2. The temperature dependence of the resonance field H_r for $\text{CdCr}_2\text{Se}_4:\text{In}$ (perpendicular geometry H_\perp , parallel geometry H_\parallel).

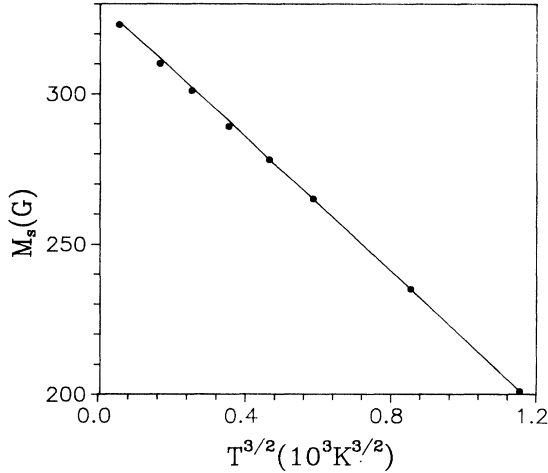


FIG. 3. The temperature dependence of the saturation magnetization M_s for $\text{CdCr}_2\text{Se}_4\text{:In}$. Solid line represents the best fit of Eq. (6).

where ξ stands for Riemann ξ -function and k_B is Boltzmann constant.

The value of B determined from the experimental data on M_s versus $T^{3/2}$ was used to calculate D from Eq. (7). We obtained $D(0) = 31.29 \text{ meV \AA}^2$. Figure 4 presents $\Delta D(T)/D(0)$ versus $T^{5/2}$ calculated from the SWR data for the same sample. The stiffness constant D scales as $T^{5/2}$ according to the spin-wave theory.¹⁰ The temperatures dependences of the resonance linewidths Γ_{\parallel} and Γ_{\perp} , in the perpendicular and parallel geometries, are presented in Fig. 5. The character of both plots is typical for the ferromagnetic spin ordering.¹¹

(ii) Reentrant transition. The reentrant transition is expected if a spin concentration is as required for the onset of the ferromagnetic spin ordering. The medium

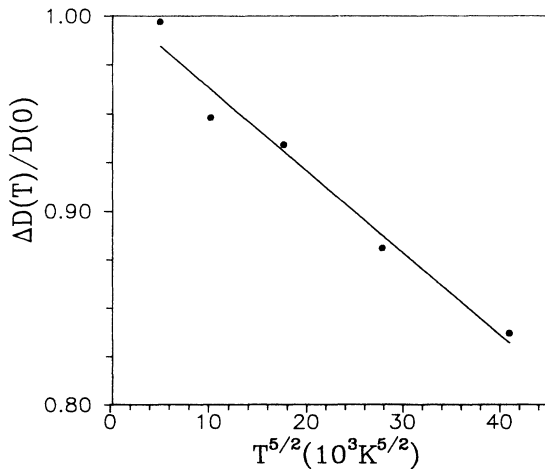


FIG. 4. The temperature dependence of the spin-wave stiffness constant $\Delta D(T)/D(0)$ for $\text{CdCe}_2\text{Se}_4\text{:In}$; $\Delta D(T) = D(0) - D(T)$. Solid line represents the linear fit to the experimental data.

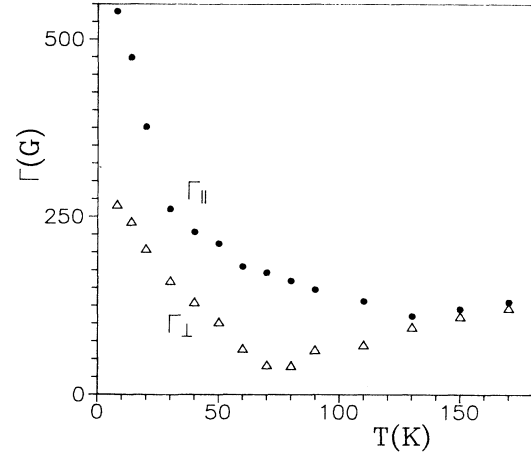


FIG. 5. The temperature dependence of the resonance linewidth for $\text{CdCr}_2\text{Se}_4\text{:In}$ (parallel geometry Γ_{\parallel} , perpendicular geometry Γ_{\perp}).

could be treated as consisting of an infinite ferromagnetic network (IFN) and finite spin clusters (FC). The intra-cluster interactions are stronger than intercluster coupling. Below the freezing temperature T_f , the ferromagnetic state becomes unstable and evolves into a spin-glass state.

The microscopic picture of the spin-glass state gives FC embedded in the sea of weakly coupled spins. In this state the effect of disorder should be the most significant. The phenomenological explanation of the transition is still far from being clear and settled.

The REE transition alters the temperature dependences of the basic magnetic parameters, hence, it affects the FMR and SWR resonance data. In the films with the REE, one expects to find the SWR only above the freezing temperature T_f , while at $T < T_f$ only the uniform mode is detected. It is the case for thin films of $\text{CdCr}_{1.9}\text{In}_{0.1}\text{Se}_4$. Figures 6(a)–6(c) present the uniform mode for $T < T_f$ ($T_f \approx 50 \text{ K}$), SWR modes for $T \geq T_f$, and for $T > T_f$, respectively. The exchange interaction constant A was calculated from the positions of volume modes [see Eq. (1)] above T_f . The value of $A = (1.6 \mp 0.2) \times 10^{-12} \text{ J/m}$ at $T = 100 \text{ K}$ is close to that characteristic for the FM state (see Fig. 1). It should be emphasized that the results of calculations are more reliable at higher temperatures because the modes become well resolved.

The temperature dependence of the saturation magnetization $M_s(T)$ was obtained from the FMR data using Eq. (5). As it is seen in Fig. 7, the experimental $M_s(T)$ deviates from the $T^{3/2}$ for $T < T_f$ ($T_f \approx 50 \text{ K}$).

The experimental results presented above can be interpreted on the basis of the model proposed in Ref. 12 and 13. The model invokes an energy gap Δ_r in the dispersion relation for magnons $E = \Delta_r + Dk^2$. That modifies the density of states and yields a nonzero density of states at the energy gap which is the fundamental feature of REE at low temperatures. The standard statistical mechanics for bosons predicts, in this case,¹²

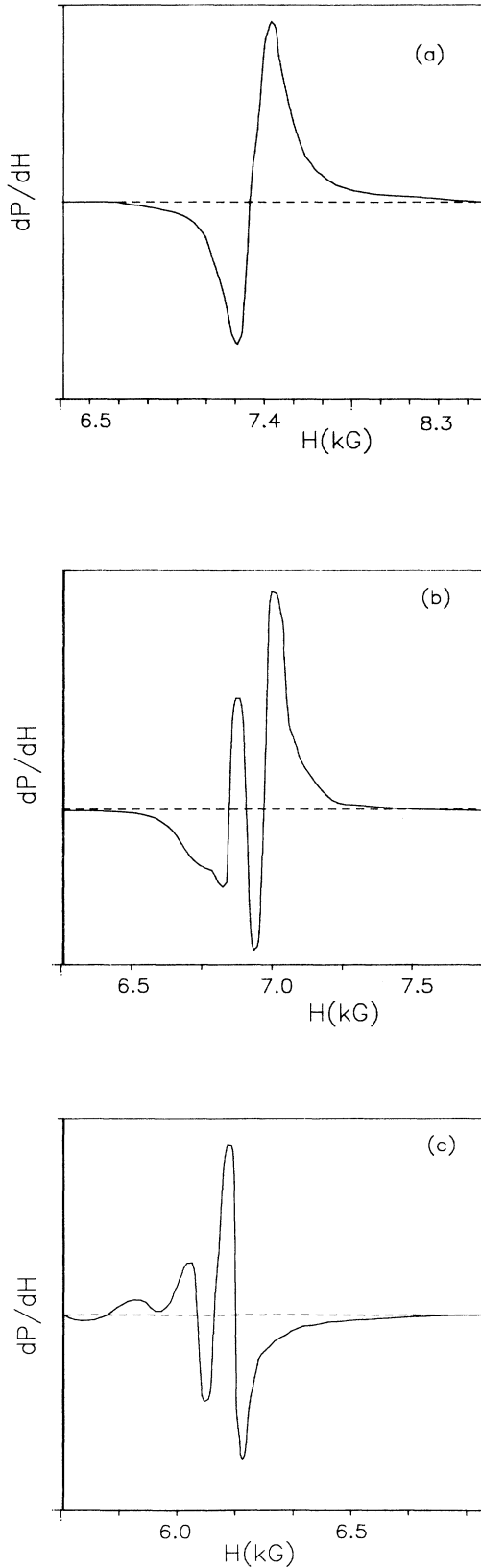


FIG. 6. Spin-wave resonance spectra for $\text{CdCr}_{1.9}\text{In}_{0.1}\text{Se}_4$ thin film at (a) $T \leq T_f$ ($T = 7.5$ K), (b) $T \geq T_f$ ($T = 55$ K), and (c) $T > T_f$ ($T = 100$ K).

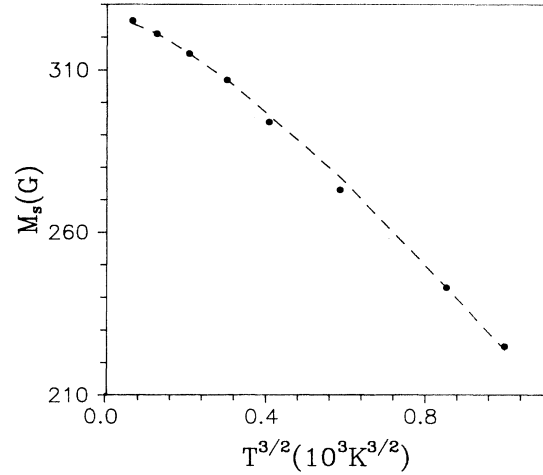


FIG. 7. M_s vs $T^{3/2}$ for $\text{CdCr}_{1.9}\text{In}_{0.1}\text{Se}_4$ thin film. Solid line represents the best fit of Eq. (8) to the experimental data with $\Delta_r = 5$ K, $T_f = 50$ K.

$$[M(0) - M_s(T)]/M(0)$$

$$= BT^{3/2}/\xi(\frac{3}{2}) \sum_{n=1}^{\infty} [\exp(-n\Delta_r/k_B T)/n^{3/2}]. \quad (8)$$

According to Eq. (8) the deviation from the classical $T^{3/2}$ law becomes more pronounced as the energy gap increases. The two-parameter fitting procedure based on Eq. (8) was employed and its results are demonstrated in Fig. 7. The $M(0)$ was taken from the extrapolation of the FMR data, Δ_r and B were treated as fitting parameters. Figure 7 shows that Eq. (8) works quite well above the characteristic temperature T_f as predicted in Ref. 12. At low temperatures ($T < T_f$), where one expects the breakdown of IFN, the model assumes δ -like density of states $\rho(E) = \delta(E - \Delta_r)$ that results in a completely different behavior of $M_s(T)$.¹³ According to the microscopic picture, given at the beginning of this section, the temperature dependence of the linewidth $\Gamma(T)$ in the SG state is expected to differ significantly from that in the ferromagnetic state. Figure 8 presents the experimental data of $\Gamma(T)$ for the $\text{CdCr}_{1.9}\text{In}_{0.1}\text{Se}_4$ thin film. Our experimental data at low temperatures can be described using the well-known analytical formula¹⁴

$$\Gamma = \Gamma_0 + \Gamma_1 (T/T_0)^n \exp(-T/T_0) \quad (9)$$

with $n = 1$. The empirical parameters T_0 and Γ_1 are found from the linear regression of $\ln[(\Gamma - \Gamma_0)/T]$ versus T . Γ_0 is the temperature-independent term. We obtained $T_0 = 12$ K, $\Gamma_0 = 110$ G, $\Gamma_1 = 537$ G for the parallel geometry, and $T_0 = 15$ K, $\Gamma_0 = 38$ G, $\Gamma_1 = 217$ G for the perpendicular geometry. It is interesting to note that both values of Γ_1 correspond quite well with those obtained by Bhagat.¹⁴ Γ_1 is very sensitive to dilution and gives the information on the interaction between the FC clusters and the long-wavelength magnons in the INF.

(iii) Spin-glass state. The concentrated spin-glass state can be microscopically illustrated as a state in which there is no IFN at all. Therefore, in the whole tempera-

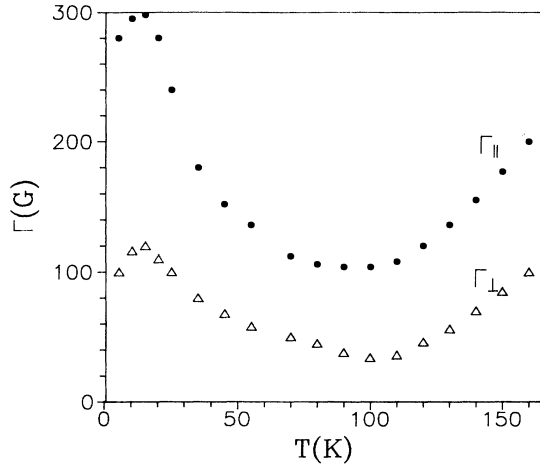


FIG. 8. Variation of the linewidth with temperature in parallel ($\Gamma_{||}$) and perpendicular (Γ_{\perp}) geometry for $\text{CdCr}_{1.0}\text{In}_{0.1}\text{Se}_4$ thin film.

ture range extending from the Weiss temperature Θ_p down to T_{SG} , which represents the characteristic temperature of spin freezing in a random direction, the dispersion relation for magnons takes a form $E = \Delta_s$, where Δ_s is the energy gap. Low spin concentration, as compared with that in the FM state, produces a strong interaction fluctuation which becomes a source of the SG phase. Theoretical understanding of such behavior and its consequences is far from being complete.

In the SG state, the temperature dependence of saturation magnetization differs distinctly from that observed in the ferromagnetic state and reentrant systems. At $T > T_{\text{SG}}$, the linear relationship between M and T is obtained, while below T_{SG} and M_s is T independent. Following the arguments presented in Refs. 12 and 13, the nonzero density of states is expected at Δ_s only. In the phenomenological picture of concentrated SG that corresponds to the breakdown of the IFN and provides for the development of separate, noninteracting spin clusters.

Therefore, the temperature dependence of the satura-

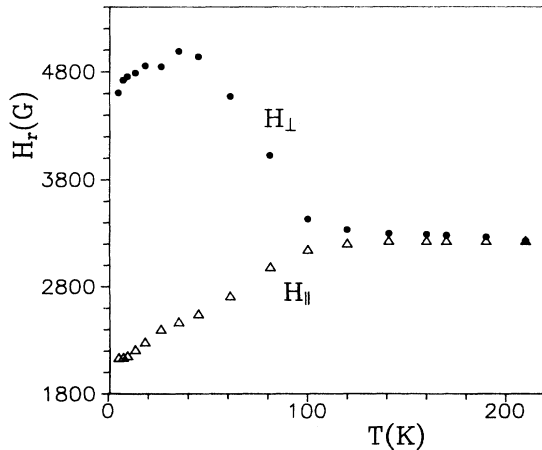


FIG. 9. The temperature dependence of the resonance field H_r for $\text{CdCr}_{1.6}\text{In}_{0.4}\text{Se}_4$ thin film.

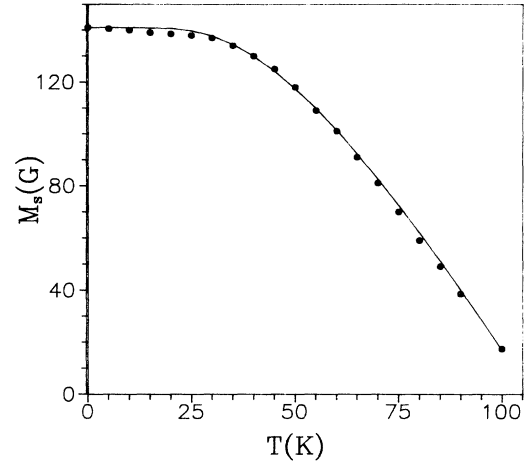


FIG. 10. Temperature dependence of M_s for $\text{CdCr}_{1.6}\text{In}_{0.4}\text{Se}_4$ thin film. Solid line represents the best fit of Eq. (12) with $\Delta_s = 145$ K, $C_s = 2.9$.

tion magnetization can be expressed as

$$[M(0) - M_s(T)]/M(0) = C_s / [\exp(\Delta_s/k_B T) - 1], \quad (10)$$

where C_s is responsible for the density of states at Δ_s and Δ_s is a measure of the intracluster interaction. This analytical formula [Eq. (10)] is also valid for REE at $T < T_f$, but with different energy gap Δ_r . It seems important to point out that, in general, Δ_s is closer to Weiss temperature Θ_p and larger than Δ_r . The temperature dependence of the resonance field H_r for the uniform mode in thin $\text{CdCr}_{1.6}\text{In}_{0.4}\text{Se}_4$ film is presented in Fig. 9.

Figure 10 shows the experimental data on M_s versus T for the same sample along with the results of the numerical analysis based on Eq. (10). From the best fit to the experimental data, two fitting parameters, Δ_s and C_s , are obtained. The value of $T_{\text{SG}} \approx 30$ K.

The temperature dependence of resonance linewidth is presented in Fig. 11 for parallel and perpendicular geometries. These results indicate the spin-glass order-

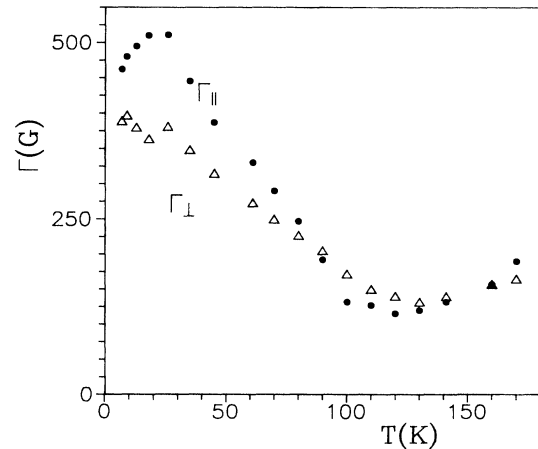


FIG. 11. The resonance linewidth Γ vs temperature T in parallel and perpendicular geometry for $\text{CdCr}_{1.6}\text{In}_{0.4}\text{Se}_4$ thin film.

ing. The low-temperature behavior of Γ is represented quite well by Eq. (9). The following values were obtained: $T_0=22$ K, $\Gamma_0=118$ G, $\Gamma_1=1191$ G for parallel geometry, and $T_0=22$ K, $\Gamma_0=135$ G, $\Gamma_1=792$ G for perpendicular geometry. All these values are of the same order as those determined for $\text{CdCr}_{2x}\text{In}_{2-2x}\text{Se}_4$ in the spin-glass state.⁶

IV. CONCLUSIONS

In this paper the magnetic properties of thin polycrystalline films of $\text{CdCr}_{2x}\text{In}_{2-2x}\text{Se}_4$ and CdCr_2Se_7 , lightly doped with In were discussed. The magnetic properties of these films were found to be very sensitive to any deviation from stoichiometry and, in particular, to In concentration. Three different magnetic types of spin ordering, i.e., the ferromagnetic state FM, the reentrant transition, and the spin-glass state were obtained in a series of samples with the intentionally varied In content (for $0.80 \leq x \leq 1.0$).

We have identified the ferromagnetic state in thin films of CdCr_2Se_4 lightly doped with In. FMR and SWR experiments carried out at the X band in the temperature range of $4.2 \leq T \leq 150$ K allowed us to determine the temperature dependences of the saturation magnetization and spin-wave stiffness constant using the boundary conditions for completely pinned surface spins.

The analytical description of the SWR and FMR was based on the semiclassical approach. We have found that the temperature dependence of the saturation magnetization $M_s(T)$ obeys Bloch's law. Thin $\text{CdCr}_{2x}\text{In}_{2-2x}\text{Se}_4$ films, with $x=0.95$, exhibit reentrant transition. The temperature dependence of saturation magnetization in that case distinctly deviates from the behavior given by the spin-wave model. The model proposed in Refs. 12 and 13 was used to account for the observed behavior of M_s . The dispersion relation for magnons was modified by including the energy gap Δ , with nonzero density of states. The analytical expression for the deviation from the $T^{3/2}$ law was found [see Eq. (8)]. It was demonstrated that Eq. (8) satisfactorily described our experimental data on $M_s(T)$ (see Fig. 7). We also observed that, for $T > T_f$, the volume modes were excited and their separation increased with temperature. The exchange interaction constant A was found.

The experimental temperature dependence of the linewidth for the parallel and perpendicular geometries is given by Eq. (9). The empirical parameters T_0 , Γ_1 , and Γ_0 were determined.

The increase in In concentration resulted in the enhanced degree of spin disorder. The spin-glass state was achieved in thin $\text{CdCr}_{2x}\text{In}_{2-2x}\text{Se}_4$ films with $x=0.8$. The temperature dependence of the saturation magnetization for samples in the SG state significantly differs from that characteristic for FM and REE. The saturation magnetization M_s is constant at low temperatures and reduces for $T > T_{SG}$, where T_{SG} is a measure of intercluster interaction. The analytical formula for $M_s(T)$ predicted in this case only exploits localized states at the energy gap Δ_s [Eq. (10)]. The energy gap Δ_s is responsible for the intracluster interaction. The satisfactory agreement between the experimental and numerical data (see Fig. 10) was obtained. The value of T_{SG} was found from the temperature dependence of the resonance field while Δ_s was used as a fitting parameter (see Fig. 10). We also should emphasize that our results of the temperature dependence of linewidth fit quite well to the universal plot $\Delta\Gamma/\Gamma_1$ versus $(T/T_0)\exp(-T/T_0)$, which is valid for a large number of alloys with randomly located spins.¹⁵

Finally, we can conclude, that in the case of the magnetic semiconductor thin Cd-Cr-Se-In films, the amount of In, very carefully controlled during deposition process, significantly modifies the magnetic properties of the material. The FMR and SWR techniques are suitable tools in the studies of the magnetic properties of such systems including coupling between spin clusters as well as the intracluster interactions.

ACKNOWLEDGMENTS

The authors are grateful to W. Powroznik from the Institute of Electronics AGH for film preparation, and Dr. R. Zuberek from the Institute of Physics of Polish Academy of Sciences in Warsaw for the FMR measurements. Thanks are also due to Dr. K. Zakrzewska from the Institute of Electronics AGH and Dr. A. Maksymowicz from the Institute of Computer Science for their contributions to the numerical analysis.

¹P. K. Baltzer, P. J. Wojtowicz, M. Robbins, and E. Lopatin, *Phys. Rev.* **151**, 367 (1966).

²M. Alba, J. Hamman, and M. Nogues, *J. Phys. C* **15**, 5441 (1982).

³M. Lubecka, L. J. Maksymowicz, R. Zuberek, and W. Powroznik, *Phys. Rev. B* **40**, 2097 (1989).

⁴M. Lubecka, L. J. Maksymowicz, and R. Zuberek, *Phys. Rev. B* **42**, 3926 (1990).

⁵S. Viticoli, D. Fiorani, M. Nogues, and J. L. Dormann, *Phys. Rev. B* **26**, 6085 (1982).

⁶D. Fiorani, M. Nogues, and S. Viticoli, *Solid State Commun.* **41**, 537 (1982).

⁷M. Lubecka and W. Powroznik, *Thin Solid Films* **174**, 71 (1989).

⁸C. Kittel, *Phys. Rev.* **110**, 1295 (1958).

⁹F. Keffer, *Handbuch der Physik*, edited by S. Fluege (Springer-Verlag, Berlin, 1966), Vol. 18, Part 2, p.2.

¹⁰J. A. Tarvin, G. Shirani, R. J. Birgeneau, and H. S. Chen, *Phys. Rev. V* **17**, 241 (1978).

¹¹J. M. Ferreira and M. D. Couthino-Filho, *J. Phys. (Paris). Colloq.* **39**, C6-1007 (1978).

¹²E. M. Jackson, S. B. Liao, S. M. Bhagat, and M. A. Manheimer, *J. Magn. Magn. Mater.* **80**, 229 (1989).

¹³S. B. Liao, S. M. Bhagat, M. A. Manheimer, and K. Moorjani, *J. Appl. Phys.* **63**, 4354 (1988).

¹⁴M. J. Park, S. M. Bhagat, M. A. Manheimer, and K. Moorjani, *J. Magn. Magn. Mater.* **59**, 287 (1986).

¹⁵K. Moorjani, S. J. Bhagat, and M. A. Manheimer, *IEEE Trans. Mag. MAG-22*, 550 (1986).